

## Structural, electronic, and magnetic properties of 3d transition-metal aluminides with equiatomic composition

J. Zou\* and C. L. Fu

*Metals and Ceramics Division, Oak Ridge National Laboratory, P.O. Box 2008, Oak Ridge, Tennessee 37831-6115*

(Received 16 May 1994)

First-principles calculations have been performed to study the chemical bonding trends and the phase stability of 3d transition-metal (TM) aluminides with equiatomic composition. The physical mechanisms for ordering in both the  $L1_0$  and  $B2$  type aluminides are presented. It is shown that the dominant factor for early TM aluminides is the directional bonding between the  $d$  orbitals of TM atoms, whereas for late TM aluminides, charge transfer and hybridization between Al  $s$  and  $p$  states and TM  $d$  states play more important roles in the bonding mechanism and the properties of lattice defects. Our calculations also show the existence of a ferromagnetic phase for MnAl in the  $L1_0$  structure, which is stabilized by the formation of a magnetic moment on the Mn sites (with a value of  $2.0 \mu_B$ ). The chemical trends in the structural stability and heats of formation of 3d TM aluminides are found to correlate well with the densities of states at the Fermi level.

### I. INTRODUCTION

3d transition-metal (TM) aluminides with (and near) equiatomic composition form important classes of high-temperature structural materials (e.g., TiAl, FeAl, and NiAl) and are promising candidates for permanent magnets (i.e., MnAl). The physical and mechanical properties of these alloys are in part determined by the atomic-level bonding interactions, i.e., the electronic structures. Phase stability and ordering behavior are two obvious examples. The fact that early TM aluminides (e.g., TiAl) form in the face-centered-tetragonal-based  $L1_0$  structure (shown in Fig. 1) and late TM aluminides (e.g., NiAl) form in the  $B2$  structure<sup>1</sup> clearly suggests that different bonding mechanisms are operating in these two ordered structures (although both classes of aluminides are intrinsically brittle). It is, thus, very important to understand this difference in the electronic structure from a materials designer's point of view, since parameters that affect the mechanical and structural properties, such as point defect structures and planar-fault energies, are dependent on the bonding characteristics.

The purpose of this paper is to investigate the structural and bonding characteristics in 3d TM aluminides. First-principles calculations are performed to determine the phase stability of these alloys. Of particular interest is the stability (and brittleness) of TiAl in the tetragonal  $L1_0$  structure. This tetragonal structure for early TM aluminides eventually evolves to the bcc-based cubic  $B2$  structure for late TM aluminides. Among these  $B2$  alloys, CoAl and NiAl are known to be strongly ordered and are deformed by anomalous  $\langle 100 \rangle$  slip<sup>2</sup> (in contrast to the  $\langle 111 \rangle$  slip for bcc-based materials); FeAl is weakly ordered and is known to be relatively ductile<sup>3</sup> (which has  $\langle 111 \rangle$  slip). The chemical bonding trends and structural stability are analyzed in terms of the electronic structures, i.e., bonding charge densities and electronic densities of states. We will show that TM-TM directional

bonding is the dominant factor governing the structural stability of early TM aluminides, while Al-to-TM charge transfer and hybridization of the electronic states play more significant roles in late TM aluminides. The degree of order is at the minimum for middle TM aluminides, which we will show is closely related to the increased density of states (DOS) at the Fermi level. The correlation between phase stability and defect properties (which affect the deformation modes and, thus, the mechanical properties of the alloys) is also discussed.

Also of great interest is the existence of a metastable ferromagnetic phase for MnAl, known as the  $\tau$  phase.<sup>4</sup> The ground state structure for equiatomic MnAl is not yet clear,<sup>5</sup> but it has been well established that a ferromagnetic phase exists near stoichiometry. This phase may be formed from the high-temperature hexagonal  $\epsilon$  phase by controlled cooling. The  $\tau$  phase has some attractive properties such as high magnetic anisotropy and moderately high magnetic energy, which make it a potential hard magnetic material. It has been shown<sup>6</sup> that the magnetic properties of the  $\tau$  phase are closely dependent on its structural properties, that is, degree of atomic order, type of crystal structure defect, etc. Thus, as a first step to understanding the  $\tau$  phase, we study the phase stability of MnAl in paramagnetic, ferromagnetic, and

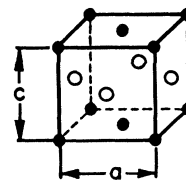


FIG. 1. Unit cell of  $L1_0$  structure, which is based on a face-centered-tetragonal lattice. The  $L1_0$  structure is equivalent to the ordered  $B2$  structure when  $c/a = 1/\sqrt{2}$ .

antiferromagnetic states. Our calculations show that the  $L1_0$  structure (or the  $\tau$  phase) is stabilized by the formation of a magnetic moment on the Mn sites, and the ferromagnetic state has the lowest energy. The calculated lattice constants and magnetic moment on the Mn sites are in good agreement with experiment.

## II. CALCULATIONAL METHOD

The calculations are based on the local-density-functional (LDF)<sup>7</sup> theory, and we use the full-potential linearized augmented plane-wave (FLAPW) method<sup>8</sup> to solve the LDF equations. The total energies of 3d TM aluminides with equiatomic composition are calculated for the ordered face-centered-tetragonal (fct) structure consisting of alternating pure Al layers and pure TM layers perpendicular to the  $c$  axis (cf. Fig. 1). Our attention is focused on two particular  $c/a$  ratios of the fct structure, i.e.,  $c/a = 1$  and  $1/\sqrt{2}$ . The ratio of  $c/a = 1$  corresponds to an fcc-based close-packed structure, where each atom has four nearest neighbors of the same type on the (001) plane and eight nearest neighbors of different type off the (001) plane. (It should be noted that, chemically, this structure is not cubic even for  $c/a = 1$ .) A typical example is TiAl, for which the  $c/a$  ratio is 1.01.<sup>1</sup> For  $c/a = 1/\sqrt{2}$ , the structure is equivalent to a bcc-based cubic structure, i.e., the ordered  $B2$  type, where each atom has eight nearest-neighbors of the other type. FeAl, CoAl, and NiAl all form in the  $B2$  structure.<sup>1</sup> We calculate the total energies for TM-Al alloys in the fct structure as functions of the  $c/a$  ratio. The preference for a certain local bonding environment for a given TM-Al alloy will be reflected in the variation of the total energy of the fct structure as the  $c/a$  ratio is changed. One unique feature of the FLAPW calculation is that no shape approximation is made to the potential or charge density, which allows an accurate determination of the energetics associated with shape deformations when  $c/a$  ratio is systematically varied from around 0.5 to 1.2. In this study, angular momentum components up to  $l = 8$  and approximately 60 plane waves per atom are used for expansion of the wave functions. The LDF equations incorporating the Hedin-Lundquist exchanged-correlation potential<sup>9</sup> are then solved self-consistently.

## III. RESULTS AND DISCUSSIONS

### A. Phase stability and electronic structure

The total energies of TiAl, VAl, CrAl, FeAl, CoAl, and NiAl alloys in the ordered fct structure are plotted in Fig. 2 as functions of the  $c/a$  ratio. (Since MnAl is found to have a large magnetic moment on the Mn sites, the interplay between magnetism and structural stability of MnAl will be discussed separately.) It shows that a structure with the  $c/a$  ratio close to 1 is more stable for TiAl, VAl, and CrAl, whereas the  $B2$  phase becomes more stable for FeAl, CoAl, and NiAl. This is consi-

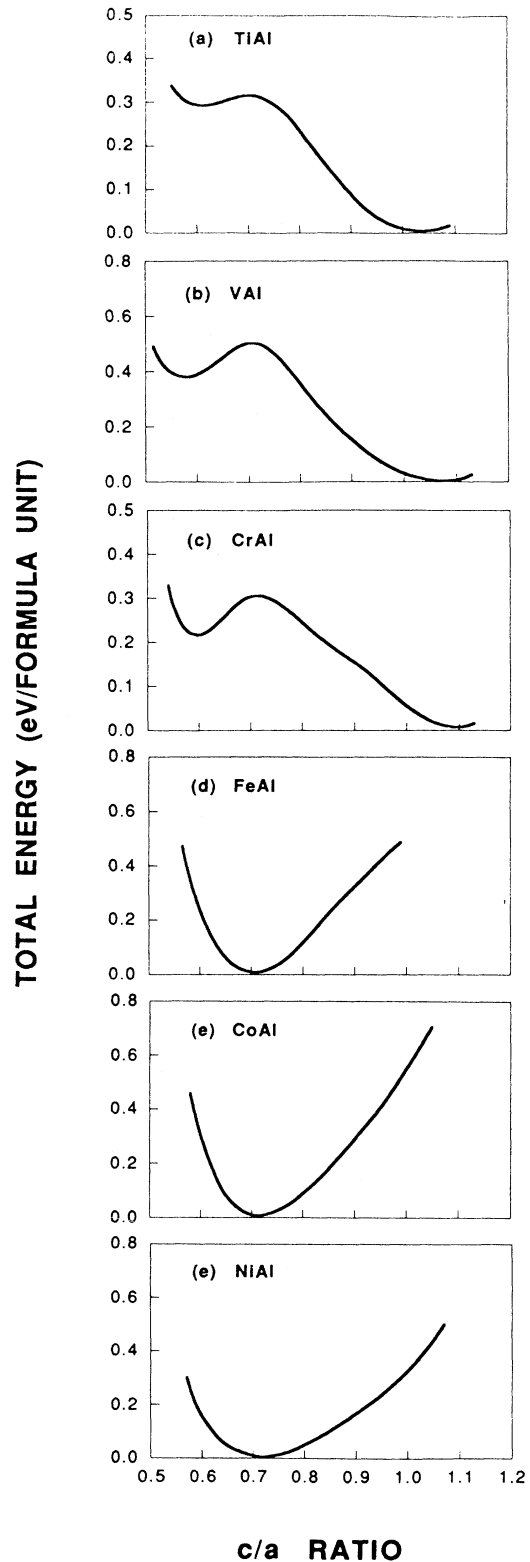


FIG. 2. Total-energy-versus- $c/a$  ratio for TM-Al in the ordered face-centered-tetragonal (fct) structure. Note that when  $c/a = 1/\sqrt{2}$ , it is equivalent to the bcc-based cubic  $B2$  phase.

tent with the observed structures of these aluminides, as TiAl indeed forms in the  $L1_0$  structure with  $c/a = 1.01$  (from now on we restrict the use of the term  $L1_0$  to those which are not cubic, i.e.,  $c/a \neq 1/\sqrt{2}$ ), and the  $B2$  phase is the ground state structure for FeAl, CoAl, and NiAl. The calculated lattice constants are in good agreement with available experimental data. Since our calculations are restricted to the ordered fct structure, the calculated lowest-energy configurations for the alloys are not necessarily their true ground states for some middle transition-metal aluminides, which are known to show the lowest degree of ordering. CrAl, for example, will phase separate into  $Al_8Cr_5$  and  $AlCr_2$  structures. (In fact, the heat of formation for  $L1_0$ -CrAl is found to be negative in our calculation.) However, we are only interested in the chemical trends in the bonding characteristics of 3d TM aluminides, instead of the exact ground state structure of a particular alloy. Thus, only the fct structure is discussed in this paper. It should be noted that there does not exist a  $B2$  phase as a metastable structure for early TM aluminides, whereas for late TM aluminides, the  $B2$  phase is the only existing stable structure as the  $c/a$  ratio is varied. The crossover between the  $L1_0$  and  $B2$  structures occurs at the vicinity of MnAl.

The origin of the structural transition from nearly fcc-based close-packed structure to the  $B2$  phase through the 3d series is the focal point of this paper. It is conceivable that this has to do with the atomic size effect. The reasoning is that the early 3d metals have atomic volumes similar to that of aluminum and a close-packed structure is favorable. On the other hand, since the atomic size difference between aluminum and transition metals increases with increasing atomic number for the 3d series, ordering in the  $B2$  phase for the late TM aluminides will reduce the strain energy due to atomic size misfit (i.e., in this structure the nearest-neighbor contacts between Al atoms are avoided). However, size effect is not the only factor that determines the phase stability of the alloys. For example, PdAl has a  $B2$  phase, in spite of the fact that Pd and Al have almost the same atomic volume. The electronic and defect properties of PdAl have been shown<sup>10</sup> to be very similar to those of NiAl, with Pd and Ni in the same column in the Periodic Table (although the atomic size mismatch between constituent atoms for these two systems is very different). This leads us to suggest that, in addition to the size effect, electronic structure should play an important role in the phase stability and other properties of TM aluminides.

To illustrate the difference in bonding characters between the  $L1_0$  and  $B2$  structures, we show in Fig. 3 the bonding charge densities, and in Fig. 4 the DOS's of VAl and CoAl, which are taken as representative examples of these two different structures. The bonding charge density is defined as the difference between the charge density in the crystal and the overlapping atomic charge density. The solid (dashed) lines in Fig. 3 denote contours of increase (decrease) electron density as the atoms are brought together to form a crystal. VAl is taken to be in the  $L1_0$  structure with  $c/a = 1.07$ . The charge density shown in Fig. 3(a) is for the (001) plane that contains V atoms only. The charge density in Fig.

3(b) is for a (110) plane of  $B2$ -CoAl, which has both Co and Al atoms.

For VAl, the dominant feature is the directional bonding between nearest-neighbor V atoms, which is expected from the open  $d$  shells of V. This is characteristic of the early 3d metals, since their  $d$  orbitals are more active than those of the late transition metals. The  $d$  orbitals of the early 3d metals are also more extended in real space, which means that nearest-neighbor  $d$ - $d$  coupling plays a more significant role. This latter point also shows how atomic size effect can be intermingled with electronic structure effect. In addition, the presence of aluminum is to introduce a noticeable multicenter bonding component among TM- $d_{x^2-y^2}$  and Al- $p_z$  states. This  $d$ - $p$  hybridization contributes to the interlayer cohesion of the  $L1_0$  structure along the  $c$ -direction. The bonding charge density of VAl is very similar to that of TiAl found previously.<sup>11</sup>

The importance of the TM-TM directional bonding is also shown in the existence of the "metastable"  $L1_0$  phases for TiAl, VAl, and CrAl, which correspond to the shallow minima in Figs. 2(a)-(c) at  $c/a \approx 0.6$ . As the

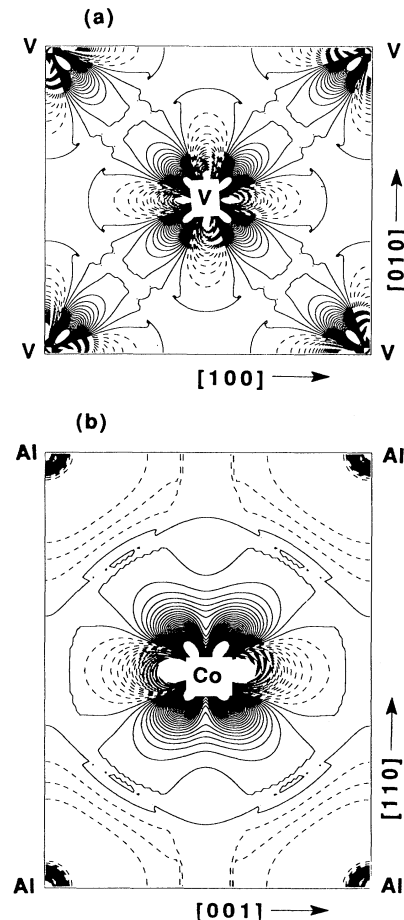


FIG. 3. Bonding charge densities in (a)  $L1_0$ -VAl and (b)  $B2$ -CoAl. The (001) and (110) planes are shown for VAl and CoAl, respectively. See text for details.

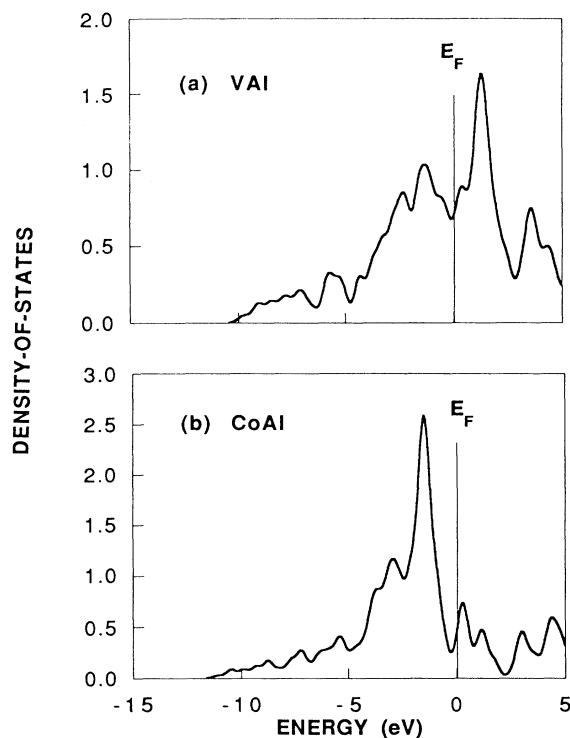


FIG. 4. Density of states (in arbitrary units) in (a)  $L1_0$ -VAI and (b)  $B2$ -CoAl. For CrAl, which has one more valence electron than VAl, the Fermi level moves to the nonbonding peak with a sharp increase in the DOS at  $E_F$ . For FeAl, which has one less valence electron than CoAl, the Fermi level is at the bonding region of the DOS profile.

$c/a$  ratios are reduced from around 1 to about 0.6 while the volume is fixed, the nearest-neighbor TM atoms in the (001) planes are getting away from each other; at the mean time, the TM atoms are moving closer to the next-nearest neighbors directly above and below them in the  $c$ -direction, until they become nearest neighbors at around  $c/a = 0.6$ . The TM-TM nearest-neighbor coordination is reduced from 4 to 2, explaining the relative stability of the two structures. The nearest-neighbor TM-TM distances in these “metastable” phases are listed in Table I, along with the equilibrium nearest-neighbor TM-TM distances in the “stable”  $L1_0$  phases represented by the deep minima in Figs. 2(a)–(c). The remarkable similarity between the two sets of numbers is a strong indication that TM-TM directional bonding dominates the structural stability of early transition-metal aluminides.

The existence of directional bonding in the  $L1_0$  struc-

ture is manifested in the well distinguished peaks and troughs in the DOS curve shown in Fig. 4(a). The first major peak below the Fermi energy ( $E_F$ ) corresponds to the directional  $d$  bonding in the pure TM (001) plane dominated by the  $d_{xy}$  states. The peak slightly lower in energy comes from the bonding states made up of TM- $d_{x^2-y^2}$  and Al- $p_z$  orbitals (interlayer bonding states). For TiAl, these states are occupied and result in the  $L1_0$  structure being the ground state. For CrAl, on the other hand, the Fermi level moves to the nonbonding peak in the DOS [the peak just above  $E_F$  for VAl in Fig. 4(a)], together with a sharp increase in the DOS at  $E_F$ . Consistent with this trend, CrAl shows the lowest degree of order among 3d TM aluminides.

As for the bonding mechanism in the  $B2$  structure, the bonding charge density of CoAl in Fig. 3(b) clearly shows a depletion of electron density at the Al sites, accompanied by a buildup of  $d$ -bonding charge at the Co sites and a slight increase of electron density in the interstitial region along the Co-Al directions. Similar bonding character is also found for NiAl.<sup>12</sup> In contrast to the  $L1_0$  structure, there is no prominent directional bonding between nearest-neighbor atoms. Obviously, there are two dominant features in the bonding mechanism of the  $B2$  structure, i.e., the long-range charge transfer (electrostatic) effect and the short-range band mixing between TM- $d$  and Al- $s, p$  states. The calculated DOS [cf. Fig. 4(b)] is dominated by the presence of TM  $d$  bands, which are found to shift away from  $E_F$  and to become narrower when the TM is alloyed with Al. This has been experimentally observed in the case of NiAl by x-ray photoelectron spectroscopy.<sup>13</sup> The DOS profile for CoAl in our calculations is also very similar to that calculated previously by Singh.<sup>14</sup> The  $d$  band is characterized by the existence of a “pseudogap” separating the bonding (between TM and Al) and nonbonding states. For CoAl and NiAl, the  $d$ -bonding states are filled (i.e., the Fermi level of CoAl is in the vicinity of the pseudogap), whereas for FeAl, the Fermi level is at the bonding region of the DOS profile.

Why is the  $B2$  phase energetically more favorable than the  $L1_0$  phase for FeAl, CoAl, and NiAl? The importance of Al-to-TM charge transfer and the filling of  $d$  bands requires that a late TM atom have as many Al atom as its nearest neighbors as possible to facilitate the charge transfer and bonding hybridization. This can be accommodated by the  $B2$  phase, where each TM atom has eight Al nearest neighbors. In the  $L1_0$  phase, the number of Al nearest neighbors to a TM atom is also 8 but the Al atoms themselves will be forced into nearest-neighbor contact. As will be discussed later, the resulting short Al-Al bonds (due to the small size of late transition-metal

TABLE I. Nearest-neighbor TM-TM distances ( $r_{nn}$ ) in the “stable” and “metastable”  $L1_0$  phases of TiAl, VAl, and CrAl.

Alloy	$(c/a)_{stable}$	$(c/a)_{metastable}$	$(r_{nn})_{stable}$	$(r_{nn})_{metastable}$
TiAl	1.03	0.60	2.76 Å	2.81 Å
VAl	1.07	0.58	2.62 Å	2.63 Å
CrAl	1.09	0.59	2.53 Å	2.59 Å

atoms) would be energetically very costly. This is the underlying physical mechanism favoring the  $B2$  phase for FeAl, CoAl, and NiAl.

### B. Heat of formation

We now discuss the heat of formation for TM aluminides. The heat of formation is a direct measure of the atomic cohesion, and is defined as

$$H(\text{TM-Al}) = E(\text{TM-Al}) - E(\text{TM}) - E(\text{Al}), \quad (1)$$

where TM and Al are in their lowest-energy states. For Al, the structure is fcc; for Ti, hcp; for V and Cr, bcc. The ground states of Fe, Co, and Ni are ferromagnetic, and fcc-Fe has a lowest energy in our calculation, although the true ground state for Fe is bcc. Co and Ni are in the hcp and fcc structures, respectively. We adopt the  $L1_0$  structure for TiAl, VAl, and CrAl, and the  $B2$  structure for FeAl, CoAl, NiAl. The calculated heats of formation are listed in Table II, along with available experiment data.<sup>15</sup>

The calculated negative heat of formation for  $L1_0$ -CrAl is consistent with the fact that CrAl phase separates into  $\text{Al}_3\text{Cr}_5$  and  $\text{AlCr}_2$  structures. The negative heat of formation obtained for ordered CrAl is partly due to the fact that Cr is a highly stable bcc metal with  $E_F$  at the valley of the bcc-DOS profile. The relatively large discrepancies in the heats of formation of FeAl, CoAl, and NiAl may be the result of the failure to find the true ground states of Fe, Co, and Ni, due to some fundamental deficiencies<sup>16</sup> in the local-spin-density approximation in treating magnetic systems.

The calculated heats of formation are also plotted in Fig. 5, which shows more clearly the chemical trend as  $d$  electron number is increased. The decrease of the heat of formation for the  $L1_0$  structure in going from TiAl to CrAl can be understood partly in terms of the relative positions of the Fermi level with respect to the bonding states in the DOS profile. As discussed in the previous section, from TiAl to CrAl, the Fermi level moves closer to the nonbonding peak in the DOS, which results in the decrease of the stability of the structure, and thus the decrease in the heat of formation. A similar argument applies to the  $B2$  structures. The major DOS peak in Fig. 4(b) corresponds to the Co  $d$  electrons of  $t_{2g}$  symmetry, hybridized with  $p$  states from Al. These are the bonding states. The small peak above the Fermi level is the nonbonding peak composed of Co  $d$  electrons of  $E_g$  symmetry. From FeAl to NiAl, the bonding states in the DOS are progressively filled, giving rise to larger heat of formation, as indicated in Fig. 5.

TABLE II. Heats of formation of TM-Al alloys (in eV/atom).

	TiAl	VAl	CrAl	FeAl	CoAl	NiAl
Ref. 14	0.39	0.18		0.26	0.56	0.61
This study	0.42	0.19	-0.11	0.32	0.65	0.68

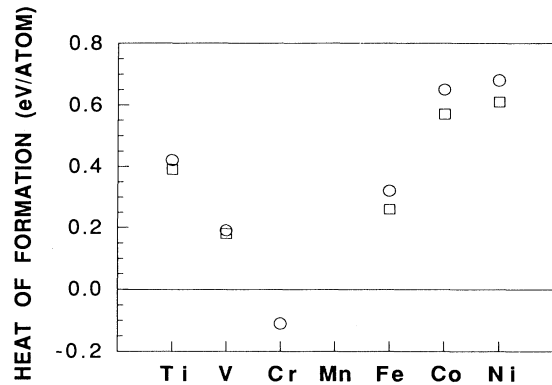


FIG. 5. Heats of formation for TM-Al alloys. Squares: experimental data from Ref. 14; circles: this study.

### C. Ordering and defect properties

The degree of order (and structural stability) is manifested in the energetics and types of defects. Previous calculations have shown that the dominant point defect types in near-stoichiometric TiAl (Ref. 11) are of antisite defects on both sublattices. This is simply due to the close-packed structure of TiAl, and the similarity in atomic size between Ti and Al. By contrast, for strongly ordered CoAl and NiAl in the  $B2$  phase, substitutional antisite defects on the Al sublattice and vacancies on the Co and Ni sublattices are found near stoichiometry.<sup>17</sup> Since the antisite defects on the Co and Ni sublattices in CoAl and NiAl would introduce nearest-neighbor Al-Al bonds, the absence of antisite defects at the TM sites indicates that short Al-Al bonds are energetically unfavorable in the  $B2$  lattice. This is partly because of the larger atomic size of aluminum than those of late 3d transition metals. Alternatively, the size effect can be viewed in terms of the embedding energy of an atom in a homogeneous electron gas. It has been shown<sup>18</sup> that aluminum atoms are stable in a rather low background electron density. On the other hand, the late transition metals require higher background densities to reach the minima of their embedding energies. Thus, the larger ( $s, p$ ) valence of aluminum suggests that the optimal way for the aluminum atoms to form an ordered alloy in the equiatomic composition with the late transition metals is to arrange themselves closer to the transition metals to facilitate the charge transfer, while keeping maximum distance from each other to maintain a lower background electron density. However, the size effect alone cannot explain adequately the presence of antisite defects at the Fe sites and the weak ordering behavior in FeAl (Ref. 17) (even though FeAl and NiAl have almost identical lattice constants). Thus, it is suggested that the electronic structure should play an important role in the ordering of  $B2$  aluminides. As the bonding states between TM and Al are occupied in CoAl [cf. Fig. 4(b)] and NiAl, the substitution of TM atoms by Al has little effect on further

enhancing the  $d$  bonding at nearest-neighbor TM sites. On the other hand, the existence of short Al-Al bonds thus introduced is energetically costly, and are prohibited by preferably creating vacancies at the TM sites. The situation is very different in the case of weakly ordered  $B2$  FeAl. In  $B2$  FeAl, antisite defects on the Fe sublattice have a much lower formation energy than in NiAl.<sup>17</sup> The Al-Al bonds thus introduced still cost energy, but this is partially compensated by the extra Al-to-Fe charge transfer (due to an extra Al atom) and the filling of more of the bonding states, since the  $d$ -bonding states are partially occupied.

The importance of the directional bonding between nearest neighbors for early TM aluminides is manifested in, for example, the large antiphase boundary (APB) energies associated with the partial  $1/2\langle 011 \rangle$  slip for TiAl,<sup>19</sup> since the APB's disrupt the nearest-neighbor bonds. Thus it is not surprising that twinning is the major deformation mode in the  $L1_0$  structure. The reason is that the boundary interface created by twinning does not alter the Ti-Al or Ti-Ti nearest neighbor bonding (the twinning energy comes from the change in bond angles between second nearest neighbors), and a low twinning energy (smaller than the APB energy by an order of magnitude) is obtained.<sup>19</sup>

That the antisite defects at the TM sites are absent in strongly ordered  $B2$  alloys is consistent with the fact that a  $\langle 111 \rangle$  slip is prohibited, since a partial  $1/2\langle 111 \rangle$  slip brings the same types of atoms into nearest-neighbor contact. Indeed, large APB energies associated with the  $1/2\langle 111 \rangle$  slip are obtained for NiAl.<sup>12</sup> Thus, the same mechanism that determines the trends in the heat of formation and degree of order also explains the increased brittleness (as a result of insufficient number of independent slips for generalized plasticity) in going from FeAl to NiAl.

#### D. Magnetic properties

For MnAl in the paramagnetic state, we find that the ordered  $B2$  phase has the lowest energy [i.e., the one with  $c/a = 1/\sqrt{2}$ , shown in Fig. 6(a)]. However, there exists a small "shoulder" in the total-energy-versus- $c/a$  curve at around 0.95 [Fig. 6(a)]. This indicates a possible metastable phase of MnAl. The DOS profile of this structure is similar to that of VAl shown in Fig. 4(a), but the Fermi level is right at the peak of the nonbonding  $d$  states. According to Stoner's criterion, this phase may well be magnetic due to the large DOS value at  $E_F$ . Thus, we have performed the spin-polarized calculation for MnAl by considering both the ferromagnetic and antiferromagnetic states. The total energy is plotted in Fig. 6(b) as a function of  $c/a$  ratio for the ferromagnetic state. Significantly, we find the existence of a ferromagnetic  $L1_0$  phase with  $c/a = 0.87$ , which is stabilized by the formation of a magnetic moment on the Mn sites. The spin-polarization energy due to ferromagnetism is calculated to be 0.30 eV per formula unit, and the magnetic moment on the Mn atoms is  $2.03\mu_B$ . The energy of

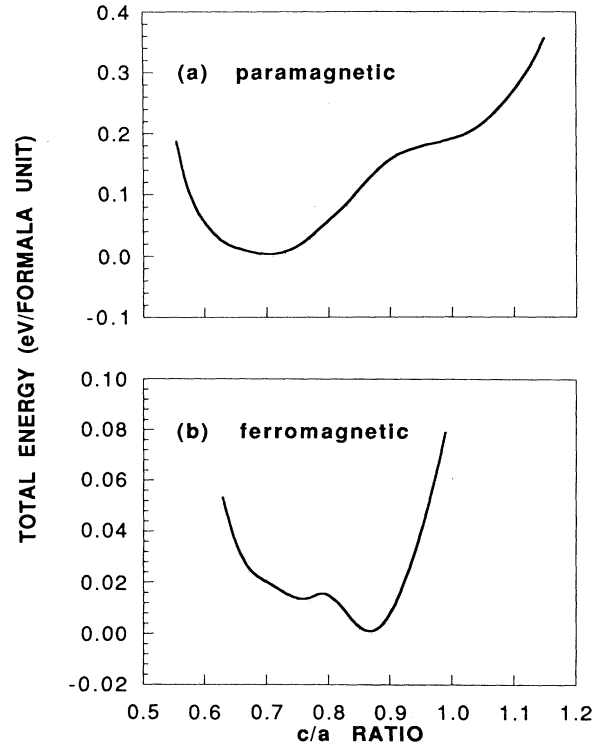


FIG. 6. Total-energy-versus- $c/a$  ratio for paramagnetic and ferromagnetic MnAl in the fct structure. The  $L1_0$  structure with  $c/a = 0.87$  becomes stable in the ferromagnetic state.

the antiferromagnetic phase is also calculated, assuming moments of opposite directions for any pair of Mn-Mn nearest neighbors. The energy is found to be between those of the paramagnetic and ferromagnetic phases. The  $B2$  phase in the ferromagnetic state, with a moment of  $1.7\mu_B$ , is no longer stable (i.e., there is no local minimum at  $c/a = 1/\sqrt{2}$  in the total-energy-versus- $c/a$  ratio curve). The existence of such a ferromagnetic  $L1_0$  phase for MnAl was actually observed in experiment<sup>4</sup> over 30 years ago. It is a metastable phase usually called the  $\tau$  phase, and is of interest as a material for permanent magnet because of its high magnetic anisotropy. The measured lattice constants and magnetic moment of this ferromagnetic phase, along with the calculated values, are listed in Table III, which shows good agreement between theory and experiment.

FeAl is also found to be ferromagnetic. However, the magnetic moment at the Fe site is found to be  $0.6\mu_B$ , which is much smaller than that of MnAl.

TABLE III. Lattice constants and magnetic moment ( $M$ ) on Mn atoms for ferromagnetic MnAl.

	$a$ (Å)	$c/a$	$M$ ( $\mu_B$ )
Ref. 4	3.92	0.90	1.94
This study	3.79	0.87	2.03

#### IV. CONCLUSIONS

We have shown in this paper that  $3d$  transition-metal aluminides are stable in the fcc-based  $L1_0$  structures for early transition metals, and in the bcc-based cubic  $B2$  structure for late transition metals. The transition from close-packed structures with nearest-neighbor TM-TM bonds to the  $B2$  structure without nearest-neighbor TM-TM contact is the result of the difference in bonding character in these alloys. For early transition metals, the atomic bonding in TM-Al is dominated by the existence of strong directional bonding between nearest-neighbor TM atoms due to the open  $d$  shells. For the late transition metals, on the other hand, Al-to-TM charge transfer and the filling of the bonding states play more important

roles. The systematic change in the  $d$ -band filling results in the variation of the structural stability and heats of formation of the alloys as the atomic number is increased. CrAl is found to have the lowest degree of order among the TM-Al alloys, and MnAl is found to be ferromagnetic. The strong ordering in CoAl and NiAl is consistent with the fact that bonding  $d$  states are filled.

#### ACKNOWLEDGMENT

This research was sponsored by the Division of Materials Science, Office of Basic Energy Sciences, U.S. Department of Energy under Contract No. DE-AC05-84OR21400 with Martin Marietta Energy Systems, Inc.

\* Present address: Department of Physics, Washington University, St. Louis, MO 63130.

<sup>1</sup> W. B. Pearson, *A Handbook of Lattice Spacings and Structures of Metals and Alloys* (Pergamon Press, Oxford, 1987), Vols. 1 and 2.

<sup>2</sup> I. Baker and P. R. Munroe, in *High-Temperature Aluminides and Intermetallics* (TMS, Warrendale, 1990), p. 425.

<sup>3</sup> C. T. Liu, E. H. Lee, and C. G. McKamey, *Scr. Metall.* **23**, 875 (1989).

<sup>4</sup> H. J. Kono, *J. Phys. Soc. Jpn.* **13**, 1444 (1958); A. J. Koch, P. Hokkeling, M. G. v. d. Steeg, and K. J. de Vos, *J. Appl. Phys.* **31**, 75S (1960); P. B. Braun and J. A. Goedkoop, *Acta Crystallogr.* **16**, 737 (1963).

<sup>5</sup> A. J. McAlister and J. L. Murray, *Bull. Alloy Phase Diagrams* **8**, 438 (1987).

<sup>6</sup> N. I. Vlasova, G. S. Kandaurova, YA. S. Shur, and N. N. Bykhanova, *Phys. Met. Metallogr. (USSR)* **51**, 1 (1981).

<sup>7</sup> P. Hohenberg and W. Kohn, *Phys. Rev.* **136**, B864 (1964).

<sup>8</sup> E. Wimmer, H. Krakauer, M. Weinert, and A. J. Freeman,

*Phys. Rev. B* **24**, 864 (1981).

<sup>9</sup> L. Hedin and B. I. Lundqvist, *J. Phys. C* **4**, 2064 (1971).

<sup>10</sup> C. L. Fu, *J. Mater. Res.* (to be published).

<sup>11</sup> C. L. Fu and M. H. Yoo, *Intermetallics* **1**, 59 (1993).

<sup>12</sup> C. L. Fu and M. H. Yoo, *Acta Metall.* **40**, 703 (1992).

<sup>13</sup> J. C. Fuggle, F. U. Hillebrecht, R. Zeller, Z. Zolnierrek, and P. A. Bennett, *Phys. Rev. B* **27**, 2145 (1983).

<sup>14</sup> D. J. Singh, *Phys. Rev. B* **46**, 14392 (1992).

<sup>15</sup> R. Hultgren, P. D. Desai, D. T. Hawkins, M. Gleiser, and K. K. Kelley, *Selected Values of the Thermodynamic Properties of Binary Alloys* (American Society of Metals, Metals Park, Ohio, 1973).

<sup>16</sup> C. S. Wang, B. M. Klein, and H. Krakauer, *Phys. Rev. Lett.* **54**, 1852 (1985).

<sup>17</sup> C. L. Fu, Y. Y. Ye, M. H. Yoo, and K. M. Ho, *Phys. Rev. B* **48**, 6712 (1993).

<sup>18</sup> K. W. Jacobsen, J. K. Norskov, and M. J. Puska, *Phys. Rev. B* **35**, 7423 (1987).

<sup>19</sup> C. L. Fu and M. H. Yoo, *Philos. Mag. Lett.* **62**, 159 (1990).